A Comparative Study of Cemented Carbide Parts Produced by Solvent on Granules 3D-Printing (SG-3DP) Versus Press and Sinter

Preprint · February 2021

CITATIONS
0

READS
82

5 authors, including:

Efrain Carreno-Morelli
University of Applied Sciences and Arts Western Switzerland
89 PUBLICATIONS **972** CITATIONS
SEE PROFILE

Patricia Alveen
Eurice GmbH
25 PUBLICATIONS **139** CITATIONS
SEE PROFILE

Steven G. Moseley
Hilti
32 PUBLICATIONS **108** CITATIONS
SEE PROFILE

Mikel Rodríguez-Arbaizar
HES-SO Valais-Wallis
36 PUBLICATIONS **212** CITATIONS
SEE PROFILE

A Comparative Study of Cemented Carbide Parts Produced by Solvent on Granules 3D-Printing (SG-3DP) Versus Press and Sinter

E. Carreño-Morelli [1], P. Alveen [2], S. Moseley [2], M. Rodriguez-Arbaizar [1], K. Cardoso [1]

[1] University of Applied Sciences and Arts Western Switzerland, Route du Rawil 47, 1950 Sion, Switzerland
[2] Hilti Corporation, 9494 Schaan, Liechtenstein

Keywords: SG-3DP, Solvent on Granules 3D-Printing, Cemented Carbides, Full Density

Abstract

Cemented carbide parts have been manufactured from WC-12Co granules by "Solvent on Granules 3D-Printing" and compared with reference parts produced by conventional press and sintering. SG-3DP consists in growing a green part layer-by-layer by selective solvent jetting on powder-polymer granule beds. Both 3D printed green parts and uniaxially pressed compacts have been consolidated by thermal debinding and liquid phase sintering. Further densification has been achieved by hot isostatic pressing.
3D-printed parts subjected to hot isostatic pressing exhibit 99.9 % of theoretical density, 1308±10 HV30 hardness and 12.1±0.3 MPa·m½ indentation toughness, which are comparable to properties of a commercial fine grained WC-12Co. Percussion drilling tests with fully dense SG-3DP drill plates have also been carried out successfully on concrete.

Introduction

The additive manufacturing (AM) of cemented carbides has been the subject of several research efforts in recent years and it is still in an early stage of development. Laser-based AM technologies have encountered several issues as thermally induced cracks, heterogeneous microstructures and embrittlement due to the formation of undesirable phases [1-2]. On the other hand, Sinter-based AM technologies offer the highest potential to process complex cemented carbide parts with properties similar to commercial grades [2-6]. This is because they are based in the growing of green bodies, which are subsequently consolidated by well-known thermal treatments already used in conventional production, which include densification by liquid phase sintering and optional improvement by hot isostatic pressing. For these techniques, limitations are related, for the moment, with layer deposition quality, part size and batch size.
Recently, Solvent on Granules 3D-Printing (SG-3DP) has been successfully used to process fully dense WC-17.7%Co complex parts [5-6]. In this paper, the feasibility of producing parts by SG-3DP with lower cobalt content is explored. The technique consists in the spreading of powder-binder granule layers, followed by selective solvent jetting. The solvent softens the binder, and the granules remain pasted to each other after solvent evaporation (Figure 1). The layer-by-layer generated green body is then consolidated by debinding and sintering [7-8]. Freedom in powder morphology and composition are among the advantages of the process, which has been successfully used for the 3D-Printing of stainless steel [9], nickel-titanium alloys [10], Invar [11], and titanium [12].

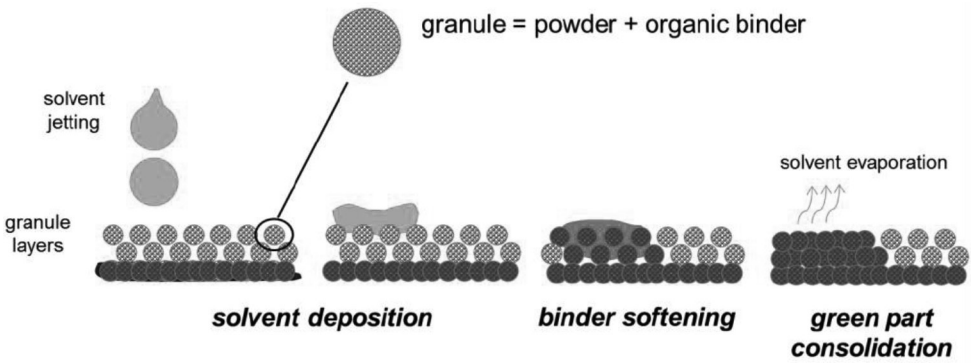

Fig. 1. Principle of Solvent on granules 3D-printing (SG-3DP)

Experimental

The base powder was a pre-sintered WC-12Co grade (Oerlikon Metco GmbH, Pfäffikon, Switzerland), which was sieved after reception to +20/-32 µm in a Sieve Shaker AS 200 apparatus (Retsch GmbH, Haan, Germany).
The powder morphology has been observed with a LEO 1525 scanning electron microscope (Carl Zeiss Inc., Thornwood, NY). Most of presintered particles are porous and round shaped. Satellites and irregular particles coming from coalescence during the production process are frequent (Figure 2a).
The powder pycnometer density of 14.17 g/cm^3 was measured with a Micromeritics AccuPyc II 1340 device (Micromeritics GmbH, Mönchengladbach, Germany).
Granules for cold compaction and 3D-Printing (WC-12Co SG-3DP granules) were processed by wet mixing the base powders with thermoplastic binder, by adding a solvent to form a slurry in a first stage. Then the slurry was dried, milled and sieved to +20/−32 µm. The resulting granule morphology is shown in Figure 2b.

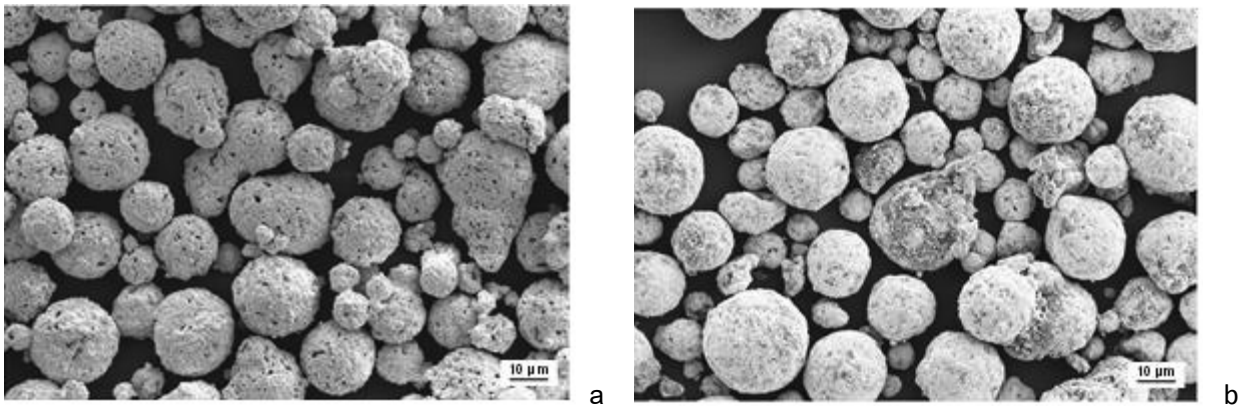

a b

Fig. 2. SEM observation of WC-12Co presintered powder (a) and WC-12Co/binder granules for compaction and 3D-Printing.

The particle size distribution of both powder and granules were determined with a Malvern Mastersizer 2000 laser diffractometer (Malvern Instruments Ltd., UK). The measured size parameters are listed in Table 1.
The bulk properties were measured according to MPIF Standards 04 and 46. The apparent density and the flow rate were measured with a Hall Apparatus (CGT - Cold Gas Technology GmbH, Ampfing, Germany) , and the tap density with a Jolting volumeter STAV II (JEL Engelsmann AG, Ludwigshafen, Germany). Density values are presented in Table 1 in g/cm^3 and as a % of the powder pycnometer density. The Hausner ratio, which is the ratio between tap and apparent densities, was calculated as a quality factor for flowability. The values for powder (1.31) and granules (1.20) are ranked as “passable” and “fair” respectively in the Hausner scale [13]. Both flow rate and Hausner ratio, show a slight improvement in flowability after granulation.
The granules were compacted in an Osterwalder CA-SP 160, 160 kN electric press (Osterwalder AG, Lyss, Switzerland), to obtain cylindrical specimens of target height 8 mm and green density in the range 40-50% of theoretical. The die was manufactured by shrink-fitting a hard metal insert into an outer tool steel die case. The punches consisted of 14.2 mm diameter hard metal punch heads brazed on steel supports. The target green density was chosen for comparison purposes, in the range of densities previously obtained in 3D-Printed green parts [5-6]. Different compaction pressures in the range 20 to 380 MPa were used.
In addition, a commercial ready to press, spray dried granule grade WC-8Co RTP (Sandvik Hyperion S.A.S., Grenoble, France) was also compacted as a reference. These granules (Figure 3) are not free flowing, and their apparent density was measured in a Carney apparatus according to MPIF Standard 28. Both apparent and tap densities are presented in Table 1 as a % of the nominal density of 14.61 g/cm^3 from the technical data sheet.

Table 1: Particle size and bulk properties of WC-12Co powder, WC-12Co granules, and WC-8Co granules

	Dv10 [µm]	Dv50 [µm]	Dv90 [µm]	Apparent density [g/cm^3]	Apparent density [%]	Tap density [g/cm^3]	Tap density [%]	Hausner ratio	Flow rate [s/50g]
WC-12Co powder	**18.7**	**24.4**	**31.2**	**4.71**	**33.2**	**6.17**	**43.5**	**1.31**	**15.8**
WC-12Co SG-3DP granules	**19.3**	**24.5**	**30.5**	**5.19**	**36.6**	**6.21**	**43.8**	**1.20**	**13.2**
WC-8Co RTP granules	2.5	54.5	123.1	3.34	22.8	4.00	27.4	1.20	NA

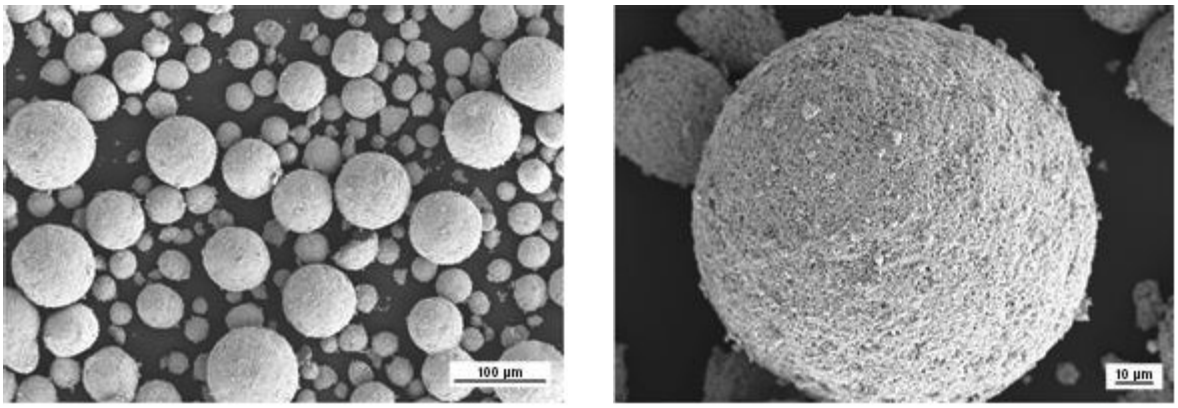

Fig. 3. SEM observation of Sandvik WC-8Co RTP spray dried granules.

The WC-12Co SG-3DP granules were used to print green parts in a special purpose SG-3DP desktop printer, which has been described elsewhere [8]. Prismatic test parts (10×10×5 mm^3) and complex shaped tools, properly upscaled to obtain the target geometries were printed. The prismatic control parts were used for density evaluation and microstructural observation. Different build jobs were performed, an example of which is shown in Figure 4.

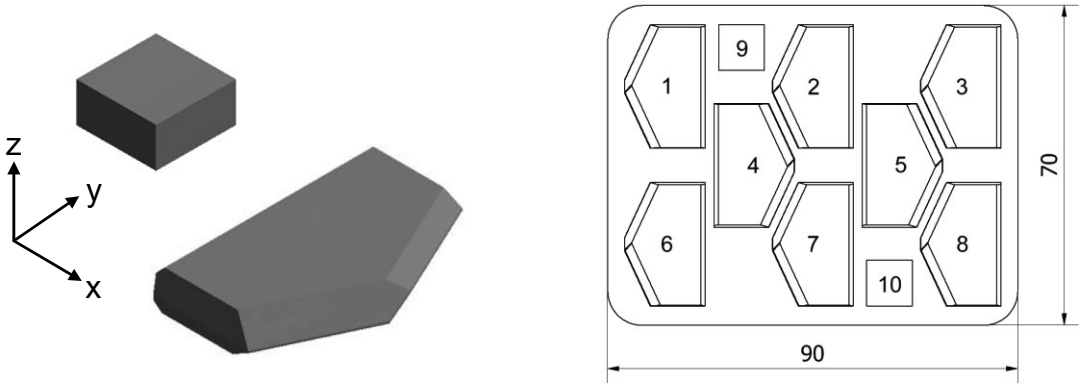

Fig. 4. Prismatic test part 10×10×5mm^3, upscaled drill plate and build job for Solvent on Granules 3DPrinting

Both the uniaxially pressed compacts and the 3D-printed green parts were debound and sintered in an ECM Lilliput graphite furnace (ECM Technologies, Grenoble, France). Boron nitride coated alumina plates were used as sintering supports. The thermal debinding was performed under nitrogen atmosphere, followed by sintering at 1420 °C for 1 h under a partial pressure of argon, which was continuously renewed with flowing gas.
In further post-processing, the sintered parts were hot isostatic pressed at 1360°C under 100 MPa argon pressure in an Abra Sinter SHIRP 8/16-200 device equipped with graphite heating elements (Abra Fluid AG, Zürich, Switzerland).
The density of green and sintered uniaxially pressed compacts and 3D-printed control prisms was determined by direct geometrical measurement. In addition, the Archimedes immersion method was used for both simple shape and complex sintered parts according to MPIF Standard 42. The porosity was estimated by optical and scanning electron microscopy according to ISO 4499-4:2016. Hardness and Palmqvist toughness measurements were carried out using a LECO V-100-C hardness tester (Leco Instrumente GmbH, Mönchengladbach, Germany) and calculated using the ISO-3878 and ASTM E1304-97 standards respectively.
Finally, the drill plates were brazed on standard helical flutes to perform percussion drilling tests on concrete by using a standard power tool under normal operating conditions.

Results and discussion

Figure 5 shows the measured compressibility curves (green density as a function of compaction pressure) for both WC-12Co SG-3DP and the WC-8Co RTP granules. Below 26 MPa the green strength of WC-12Co SG-3DP compacts is reduced, and it becomes difficult to avoid cracking during ejection from the die.

The compressibility of SG-3DP granules is low compared to the commercial RTP granules (Figure 5). This is due to differences in the granule size distributions, the binder type and content, and the fact that SG-3DP granules are based on pre-sintered powder. Nevertheless, the sintered density and linear shrinkage of compacts are equivalent in the same range of green densities, as shown in Figures 6a and 6b, which demonstrates that the WC-12Co granules are suitable for producing dense parts.

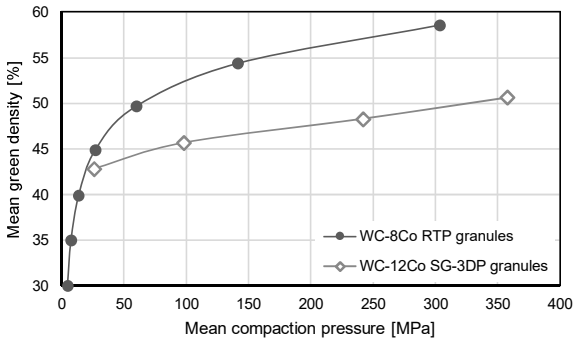

Fig. 5. Compressibility curves of WC-12Co SG-3DP granules and WC-8Co RTP granules

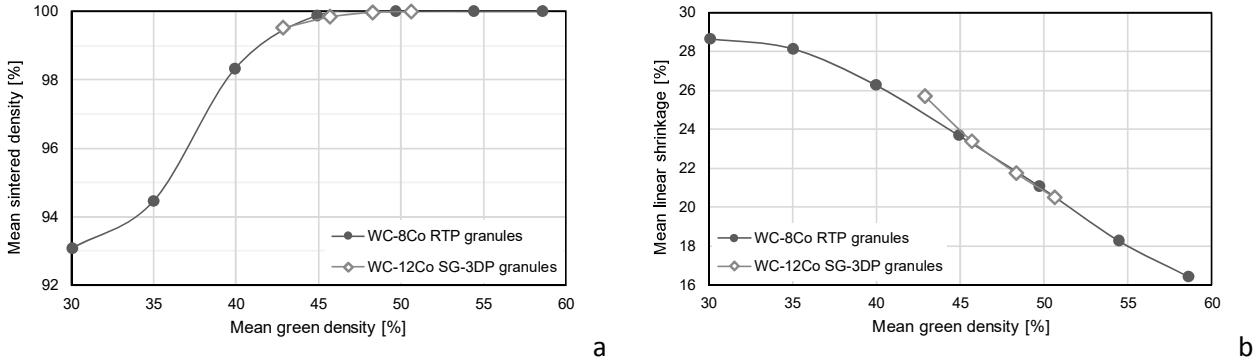

Fig. 6. Comparison of mean sintered density and linear shrinkage as a function of green density for WC-12Co SG-3DP and WC-8Co RTP granules (each dot is an average of 3 samples)

Figure 7a shows an example of green and sintered WC-12Co test parts. Figure 7b shows the sintered microstructure obtained for a part compacted at the lowest pressure of 26 MPa, which results in a green density similar to the one obtained with the SG-3DP process. Full sintered density is reached for compaction pressures higher than 240 MPa and green densities higher than 48% of the powder pycnometer density.

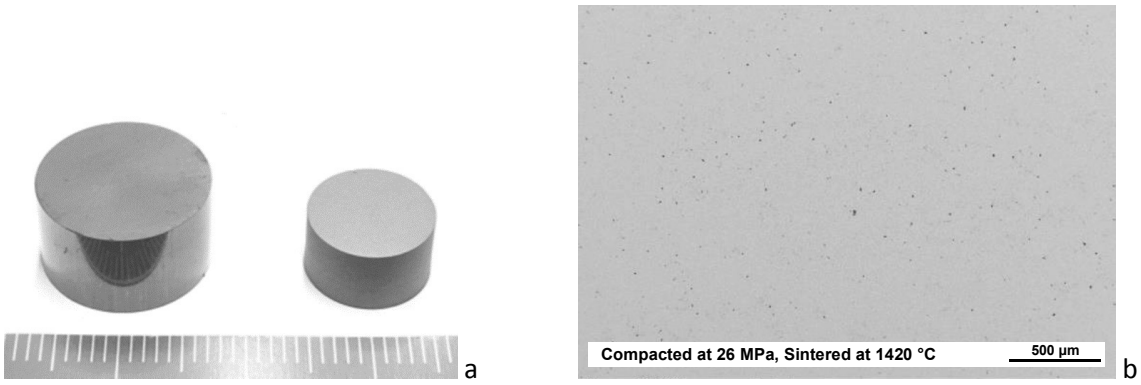

Fig. 7. Press and sintered WC-12Co parts (a), and SEM picture of a 99.5% dense sintered microstructure (b)

Figure 8 shows a setup of two SG-3DP build jobs on its sintering support before and after sintering. The mean green density is 39.9% of powder pycnometer density. Sintered parts exhibit good shape retention, mean shrinkages in the range 24% to 26% depending on direction and mean sintered densities of 97.4%. The residual porosity of 2.6% can be seen in Figure 9a.

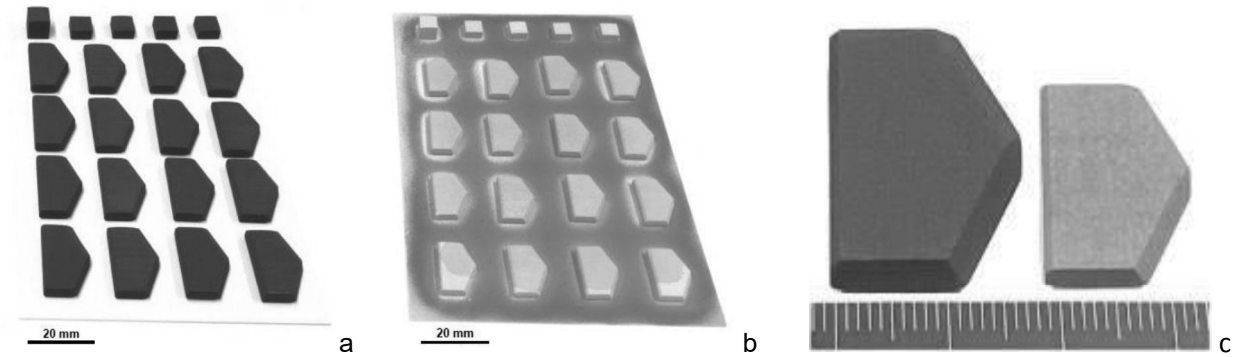

Fig. 8: Set of green (a) and as-sintered (b) WC-12 Co parts on its sintering support. Comparison between green and sintered WC-12 Co drill plates (c)

Hot isostatic pressing allowed full densification (Figure 9b). The parts exhibit B04 porosity (pore size between 10 and 25 µm, ISO 4499-4). High magnification images show inhomogeneities in cobalt distribution, as pools resulting from cobalt squeezing into the pores of the as-sintered microstructure. The overall linear shrinkage after HIP was between 24.5% and 26.5% compared with the green dimensions, with a maximum observed in the z direction (the normal to the granule layer x-y plane). The measured hardness was 1308±10 HV30 and the Palmqvist indentation toughness was 12.1±0.3 MPa·m½, which is similar to known values for a commercial fine-grained WC-12Co material produced using a conventional press and sinter route. Preliminary transverse rupture strength (TRS) measurements have shown scattered results, with average values slightly below those of conventional reference hard metal. This suggests that further improvement is necessary to reduce residual porosity and obtain a more uniform cobalt mean free path.

Table 2 summarizes values of green density and overall shrinkage (average of 10 reference prismatic parts), as-sintered and HIPed densities (average of 51 parts), corresponding to five WC-12Co SG-3DP build jobs.

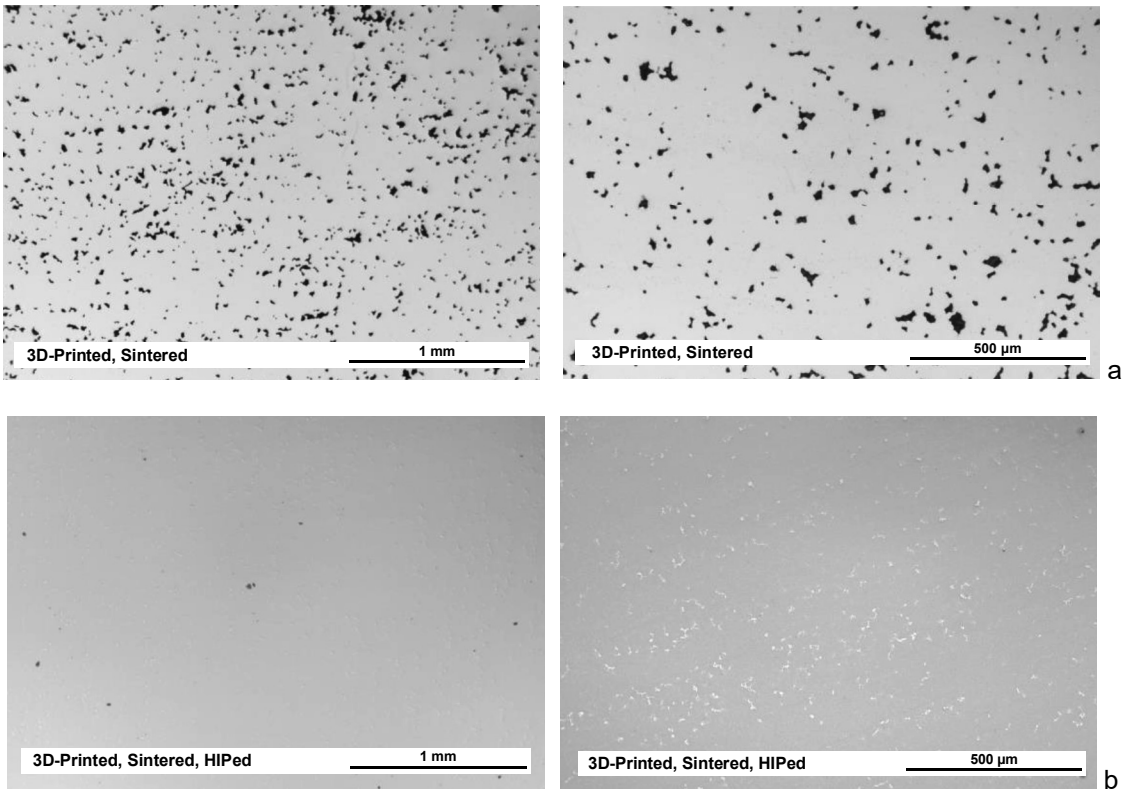

Fig. 9: Optical microscopy of 3D-printed WC-12Co, as sintered (a) and after densification by HIP (b)

Table 2. Archimedes density and mean overall linear shrinkage of 3D-Printed WC-12Co

green density		sintered density		HIPed density		overall linear shrinkage		
[g/cm^3]	[%]	[g/cm^3]	[%]	[g/cm^3]	[%]	x [%]	y [%]	z [%]
5.65	39.9	13.80	97.4	14.16	99.9	24.5	25.4	26.5

The measured magnetic saturation was about 1.8 µT.m^3.kg^{-1}, which meets values for regularly processed WC-12Co hardmetal and confirms the absence of free carbon and eta-phase. The coercive force measured according to ISO 3326 Standard was about 10 kA.m^{-1}, which corresponds to fine grained (~1 µm) WC-12Co [14].
Preliminary percussion drilling tests performed with HIPed drill plates brazed on standard flutes were successful (Figure 10). A series of 20 consecutive drillings on C50/60 concrete with hole depths of 80 mm showed that the plate geometry and cutting-edges integrity were satisfactory, with no broken plates, good hole quality and capacity for extensive additional drilling. Additional lifetime testing is in progress.

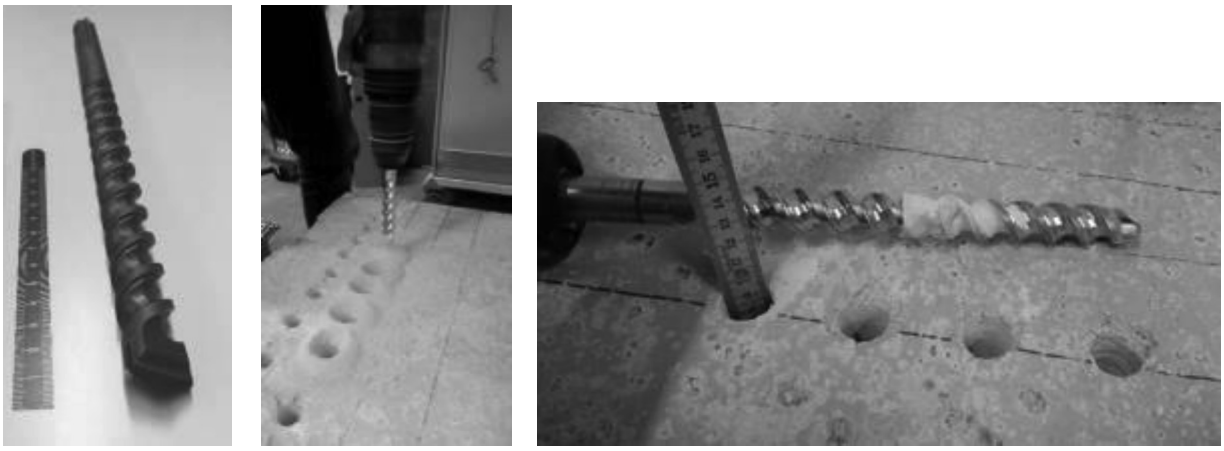

Fig. 10: SG-3DP drill plate brazed on helical flute and percussion drilling test

Conclusions

WC-12Co / binder granules have been prepared from presintered powder. The granules were suitable for both Press and Sintering, and Solvent on Granules 3D-Printing.

Solvent jetting on granule beds, followed by debinding, liquid phase sintering and hot isostatic pressing allowed to produce fully dense hard metal parts with good shape retention. The resulting microstructure, hardness and toughness are close to those of press and sintered parts obtained by the conventional route.

Functional WC-12Co drill plates for concrete percussion drilling have been successfully 3D-printed, consolidated, brazed on standard helical flutes, and tested.

Acknowledgments

Authors grateful acknowledge Innosuisse, the Swiss Innovation Agency, for its support through Grant 28800.1 IP-ENG (2018–2021).

References

1. E. Uhlmann, A. Bergmann, W. Gridin, Procedia CIRP 35 (2015) 8‑15.
2. A. Mostafaei, A.M. Elliott, J.E. Barnes, C.L. Cramer, P. Nandwana, M. Chmielus, Progress in Materials Science (2020), doi: https://doi.org/10.1016/j.pmatsci.2020.100684
3. J. Pötschke, C. Berger, H.-J. Richter, U. Scheithauer, S. Weingarten, Proc. of European Powder Metallurgy Congres EuroPM2017, 1‑6.
4. M. Kitzmantel, W. Lengauer, I. Duretek, V. Schwarz, C. Kukla, C. Lieberwirth, V. Morrison, T. Wilfinger, E. Neubauer, Proc. of 2018 World Conference on Powder Metallurgy, pp. 938‑945.
5. E. Carreño-Morelli, P. Alveen, S. Moseley, M. Rodriguez-Arbaizar, K. Cardoso, Proc. of 11th Int. Conf. on the Science of Hard Materials ICSHM11, Khao Lak, Thailand, March 25-29, 2019, pp. 1-2

6. E. Carreño-Morelli, P. Alveen, S. Moseley, M. Rodriguez-Arbaizar, K. Cardoso, Int. Journal of Refractory Metals and Hard Materials, 87 (2020) 105110
7. E. Carreno-Morelli, S. Martinerie, J.-E. Bidaux, Granules for three-dimensional printing, European patent application EP05109045. (2005) 4.
8. E. Carreno-Morelli, M. Rodriguez-Arbaizar, G. Flueckiger, C. Cachelin, F. Bircher, J. Renner, J. Richard, Proc. of World Conference on Powder Metallurgy WorldPM2016, Hamburg, Germany, October 9-14 (2016), pp. 1‑6.
9. E. Carreño-Morelli, S. Martinerie, L. Mucks, B. Cardis, Mater. Sc. Forum 591-593 (2008), pp.374-380
10. E. Carreño-Morelli E., J.-E. Bidaux, Advances in Powder Metallurgy & Particulate Materials - 2008, Metal Powder Industries Federation, 2008, pp. 4.191-4.199
11. E. Carreño-Morelli, M. Rodriguez-Arbaizar, H. Girard, Proc. of European Powder Metallurgy Congress EuroPM2018, Bilbao, Spain, October 14-18, 2018, pp.1-6
12. E. Carreño-Morelli, M. Rodriguez-Arbaizar, K. Cardoso, A.B. Nagaram, H. Girard, S. Rey-Mermet, Int. Journal of Refractory Metals and Hard Materials, 92 (2020) 105276
13. R.O. Grey, J.K. Beddow, Powder Technol. 2 (1969) pp. 323‑326
14. A. Love, S. Luyckx, N. Sacks, Journal of Alloys and Compounds. 489 (2010) pp. 465–468